Taylor & Francis
Taylor & Francis Group

Cogent Engineering

ISSN: 2331-1916 (Online) Journal homepage: www.tandfonline.com/journals/oaen20

Optimizing LoRaWAN throughput in maritime environments through adaptive coding and modulation in Rayleigh fading channels

Martine Lyimo, Bonny Mgawe, Judith Leo, Mussa Dida & Kisangiri Michael

To cite this article: Martine Lyimo, Bonny Mgawe, Judith Leo, Mussa Dida & Kisangiri Michael (2026) Optimizing LoRaWAN throughput in maritime environments through adaptive coding and modulation in Rayleigh fading channels, Cogent Engineering, 13:1, 2664960, DOI: 10.1080/23311916.2026.2664960

To link to this article: https://doi.org/10.1080/23311916.2026.2664960

Published online: 01 Jun 2026.

COGENT ENGINEERING
2026, VOL. 13, NO. 1, 2664960
https://doi.org/10.1080/23311916.2026.2664960

ELECTRICAL AND ELECTRONIC ENGINEERING | RESEARCH ARTICLE

OPEN ACCESS Check for updates

Optimizing LoRaWAN throughput in maritime environments through adaptive coding and modulation in Rayleigh fading channels

Martine Lyimo, Bonny Mgawe, Judith Leo, Mussa Dida and Kisangiri Michael

School of Computational and Communication Science and Engineering, The Nelson Mandela African Institution of Science and Technology, Arusha, Tanzania

ABSTRACT

This article proposes an Adaptive Coding and Modulation (ACM) scheme to improve the throughput of Long-Range Wide Area Network (LoRaWAN) in a maritime environment where wireless communication faces severe challenges from multipath propagation, interference, and Rayleigh fading. Unlike conventional LoRaWAN systems that use fixed physical layer configurations, dynamic adjustment of spreading factor (SF), coding rate (CR), and bandwidth (BW), according to channel conditions based on real-time Signal-to-Noise Ratio (SNR), is another solution to respond to communication challenges in the maritime environment. Simulations using a Rayleigh fading model with six different configuration levels demonstrate that the proposed ACM can achieve a gain of up to 10^3 times the throughput improvement compared to fixed SF7 under low SNR conditions while maintaining link reliability. This work establishes the foundation for implementing efficient and reliable LoRaWAN networks in maritime Internet of Things (IoT) applications.

ARTICLE HISTORY
Received 5 August 2025
Revised 20 January 2026
Accepted 16 March 2026

KEYWORDS
LoRaWAN; maritime IoT; Rayleigh fading; adaptive modulation; physical layer adaptation; signal processing; low power wide area networks (LPWAN)

SUBJECT
Electrical & Electronic Engineering; Wireless Communication; Signal Processing; IoT; Maritime Systems

1. Introduction

Wireless signal transmission in the systems is disturbed by path loss, fading, noise, and interference. These degradations are even more significant in an open maritime environment, which includes multipath reflections and time-varying channel conditions, resulting in poor signal quality and degraded link reliability (Xylouris et al., 2024). While maritime IoT use cases pose unique communication challenges, they are particularly well-suited for environmental sensing, offshore facility management, and related applications (Durlik et al., 2023). Most of these applications require an end-to-end link that can withstand varying maritime environment conditions (Liu et al., 2023). Traditional fixed-parameter techniques are not able to offer stable results in different maritime environment cases, from calm seas with a clear Line of Sight (LoS) to bad weather and a strong multipath environment (Pinelo et al., 2023).

LoRaWAN, a common LPWAN protocol, enables long-range, low-power, and reliable communication through Chirp Spread Spectrum (CSS) modulation and the physical layer (PHY) (Maleki et al., 2024). Most of the LoRaWAN deployments work with static physical layer configurations like fixed SF, CR, and BW. This static characterization restricts adaptability and can adversely affect throughput as well as link robustness, particularly under fading conditions that occur frequently in maritime environments (Ruotsalainen et al., 2022).

Although the standard LoRaWAN Adaptive Data Rate (ADR) allows some parameter adaptation, it mainly addresses SF adaptation according to long-term network statistics, which is not applicable in dynamic maritime environments (Al-Sammak et al., 2025). The proposed approach differs from fixed

CONTACT Martine Lyimo martine.lyimo@nm-aist.ac.tz School of Computational and Communication Science and Engineering, The Nelson Mandela African Institution of Science and Technology; P.O. Box 447, Arusha, Tanzania

configuration as it performs full SF, CR and BW adaptation as a function of real-time per-channel feedback, which allows it to react much faster to variations in the channel. In contrast to recent machine learning (ML) driven techniques, which need a large amount of training data and computation resources (Maurya et al., 2025), the proposed SNR-based method provides an efficient solution that can easily be embedded into resource-constrained IoT devices.

LoS is commonly encountered in wireless communication, but for practical situations, such as near-shore systems, low height of the antenna, and unfavourable weather, multipath fading could be quite severe. To fairly model these worst-case scenarios, Rayleigh fading is usually applied since it can be used to model the multipath environment where there is no direct LoS (Haq et al., 2025).

The proposed ACM technique is optimized for slowly varying Rayleigh channels, such as those that can be experienced in maritime sites. It makes use of channel estimation at the receiver to aid the adaptation at the transmission level; hence, it can achieve good efficiency and adaptability in radio resource utilization. Based on the context, this article evaluates the benefit of ACM configuration over the fixed configuration under various SNR scenarios.

1.1. Problem formulation

Maritime environments present significant wireless communication challenges due to multipath propagation, interference, and Rayleigh fading (Xylouris et al., 2024; Pinelo et al., 2023). In marine wireless communications, radio signals are greatly attenuated and scattered by weather conditions, such as rain, fog, and wind, especially for long-range maritime links (Li et al., 2023; Wang et al., 2023). The multipath effect also occurs at the surface of the sea, caused by reflections from the sea surface, waves, and vessels, resulting in delayed and interfering signal replicas, which corrupt the reception and introduce symbol interference (Alqurashi et al., 2022). These effects combine to contribute to the Rayleigh fading effects, where the received signal strength varies rapidly in amplitude and phase due to the absence of a strong LoS component, making connections at sea challenging to maintain (Cheng and Wang, 2025). These conditions severely affect LoRaWAN performance under fixed configurations (Liu et al., 2023) and multiple transmission sources all contribute to signal fading and instability in maritime wireless communication systems. The main propagation impairments in maritime wireless communication, including multipath fading, reflection, and shadowing, are illustrated in Figure 1 (Lyimo et al., 2026).

This work addresses the challenge of maintaining reliable communication while optimizing throughput in changing maritime conditions. The goal is to improve LoRaWAN throughput in maritime environments by using adaptive configuration techniques. This optimization is achieved through the following methodology;

- Define a collection of discrete PHY levels using different (SF, CR, BW) pairs.
- Performance simulation of Packet Error Rate (PER) for each PHY level under Rayleigh fading.
- Include the frame retransmissions and calculate the effective throughput for different scenarios.
- Simulation of the developed SNR-based ACM algorithm and comparison with static configurations and ADR/ADR-Enhanced.

1.2. Research contributions

The most important contribution of this article to the literature on maritime wireless communication and LoRaWAN performance analysis can be summarized as follows:

- It proposes an adaptive coding and modulation ACM strategy for LoRaWAN to choose the best performance SF, CR and BW values through real-time SNR feedback applied for marine channel conditions.
- It provides an extensive simulation environment that accounts for Rayleigh fading, LoRa PHY specifics, and a stop-and-wait feedback mechanism to emulate practical maritime communication scenarios.

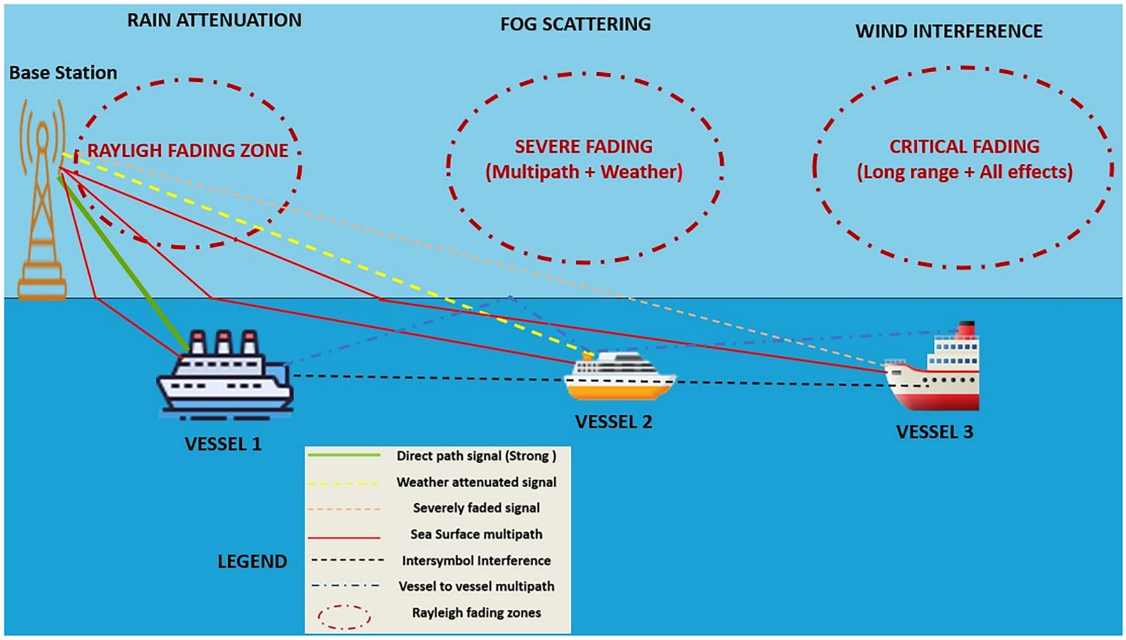

Figure 1. Propagation impairments in maritime wireless communication (Lyimo et al., 2026).

- The scheme is shown to outperform a counterpart with fixed parameters through a quantitative performance evaluation based on Monte Carlo simulations, with throughput gains of up to 1000× at low SNR.
- It evaluates the energy and spectral efficiency performance of the ACM scheme in a wide SNR range. It demonstrates that ACM performs well for both power and bandwidth-limited maritime IoT.
- It compares the proposed method systematically against some fixed and adaptive algorithms (ADR/ADR-Enhanced) and concludes its suitability to dynamic and interference-rich marine environments.

The rest of the article is organized as follows, where Section 2 is about related work on LoRaWAN adaptation in the maritime environment. The methodology is explained in Section 3, including the system model, simulation framework, and SNR-based ACM algorithm. Section 4 reports the results and discussion on the findings from simulations. Section 5 discusses future work, and the article is concluded in Section 6.

2. Literature review

Although there have been several studies about LoRaWAN in a maritime environment, little attention has been given to the need for dynamic adaptation. For instance, Li et al. (Li et al., 2024) created a LoRa-based maritime positioning system using fixed parameters, which meant it couldn't adapt to changing conditions at sea. Similarly, Li et al. (Li et al., 2023) focused on modelling the ship-to-ship channel in different maritime conditions but did not deploy adaptive schemes to adapt to such changes.

Parri et al. (Parri et al., 2019) achieved long-distance maritime transmission with fixed parameters and dedicated antennas. Still, their method could not adjust to the change of weather or minimum power usage for different environments. Due to their fixed CR (4/5) and SFs, they provided more limited opportunities to improve performance in challenging conditions.

Researchers have also used adaptive methods, but not specifically for maritime applications. Teymuri et al. (Teymuri et al., 2023) designed LoRaWAN adaptation in urban areas with reinforcement learning, and Farhad et al. (Farhad et al., 2020) presented the G-ADR algorithm for improving the mobile LoRaWAN. However, these solutions are not tailored to the specific challenges of maritime environments.

Guerra et al. (Guerra et al., 2024), looked at how weather impacts LoRaWAN and created models to predict signal strength from different weather factors. They did not, however, use any adaptive configurations to adjust the system based on these predictions. Pensieri et al. (Pensieri et al., 2021) presented very useful real-world evidence of long-range maritime LoRa transmissions. Still, they depended on general ADR schemes that mainly provide parameter adaptation according to the long-term statistics and consider mainly the SF adaptation rather than exploiting special maritime adaptations.

Recent studies increasingly explore learning-based optimization for LoRa/LoRaWAN and maritime IoT systems to improve reliability, energy efficiency, and latency under dynamic conditions. For example, multi-armed bandit and reinforcement-learning approaches have been proposed to enhance LoRaWAN parameter selection beyond the rule-based ADR mechanism, aiming to improve energy efficiency and packet delivery in changing environments (Almarzoqi et al., 2022). Deep learning–based ADR mechanisms have also been proposed to improve reliability while maintaining low power consumption in dense and dynamic networks (Leonardi et al., 2025). In parallel, maritime edge computing and task offloading frameworks, such as VESBELT, address energy–latency trade-offs in Maritime IoT, highlighting the broader trend toward adaptive, intelligent optimization in marine networks (Ghoshal et al., 2024). These works motivate lightweight adaptation mechanisms, such as the proposed ACM, while our focus remains on PHY-level parameter adaptation under fading to improve throughput.

Other related work has examined modifications to the standard ADR procedure and adaptive parameter selection outside the LoRaWAN protocol. Enhanced ADR variants adjust the original decision rules to improve convergence behaviour in terrestrial networks, but operate only on the spreading factor and assume slowly varying channel conditions (Al-Gumaei et al., 2022). In a different context, adaptive LoRa schemes such as Allora adjust physical-layer parameters under simplified channel assumptions; however, these approaches are not designed for LoRaWAN operation and do not account for regulatory constraints, feedback mechanisms, or maritime fading (Arratia et al., XXXX).

The proposed approach addresses this gap by developing an ACM framework tailored for maritime LoRaWAN deployments. Compared with the conventional techniques, the proposed system adjusts SF, CR and BW dynamically according to the real-time channel state information, resulting in a much faster response to varying conditions. Table 1 compares existing works and the proposed approach.

3. Methodology

This section highlights how the proposed ACM algorithm for improving LoRaWAN throughput is achieved, as described in the problem formulation section.

3.1. Maritime propagation scope and assumptions

This study focuses on small-scale fading effects representative of maritime multipath dynamics by modelling the channel as Rayleigh fading (with additive noise) to evaluate the benefits of rapid PHY reconfiguration. We acknowledge that real maritime propagation may include additional large-scale and deterministic components such as two-ray sea-surface reflection, evaporation ducting/ducted propagation, weather-dependent attenuation, and variability due to sea state (wave height) and humidity. These factors can alter the instantaneous and long-term SNR distribution and may shift the optimal switching thresholds. Incorporating these sea-specific propagation mechanisms into the channel model and validating the scheme using measurement-driven maritime datasets are planned for future work.

3.2. LoRa modulation and coding parameters

Table 2 summarises the predetermined PHY configuration levels employed in the ACM. Each level uses a unique combination of SF, CR and BW, while a higher BW (250 kHz) for SF7 is used to achieve as high a data rate as possible in high SNRs, and 125 kHz for SF8–SF12. Coding rates are more robust at higher SFs, helping maintain reliability in harsh channels. All setups use a fixed payload of 100 bytes for fair comparison, and the corresponding Time-on-Air (ToA) is calculated at each level. Level 6 (SF12) acts as a fallback to work at low SNR and, therefore, provides more robustness to the link in deep fading

Table 1. Summary of related works.

References	Environment	Adaptation	Channel model	Key contribution	Identified gap
(Li et al., 2024)	Maritime	Fixed parameters	Empirical, measurement-based approach	Maritime position-indicating beacon system	No adaptation for channel variations
(Li et al., 2023)	Maritime	Fixed parameters	Round Earth Loss (REL)	Channel modelling between ships in different maritime settings	No adaptive configuration
(Parri et al., 2019)	Harsh offshore maritime	Fixed CR (4/5) with different SF	Wireless fading and path loss models with Fresnel zone consideration	Demonstrated reliable long-distance maritime transmission using LoRaWAN fixed parameters and antenna	No dynamic adaptation of CR; longer packets increase time on air and power consumption; possible performance loss in weather changes not tested
(Teymuri et al., 2023)	Urban and suburban	ADR	LoRaLogNormalShadowing	Reinforcement learning for ADR	Not maritime-focused, configuration flexibility trade-off
(Farhad et al., 2020)	Mobile IoT	ADR	Gaussian Filter-Based ADR (G-ADR)	Shortening the convergence time while enhancing the packet's success ratio of mobile LoRaWAN devices	No maritime concentration, not nimble enough to change to different channels quickly
(Guerra et al., 2024)	Outdoor terrestrial environment	Weather-dependent time-varying channel	Empirical path loss	Received Signal Strength Indicator (RSSI) prediction incorporating weather variables	No adaptive configuration
(Pensieri et al., 2021)	Maritime	ADR	free-space LoS	Offers strong empirical evidence for long-range maritime IoT data transmission	Environment-induced path loss
(Pinelo et al., 2023)	Maritime	Fixed Parameters	Empirical	Performance factors in maritime LoRaWAN	No adaptation strategies
(Bagwari et al., 2022)	Terrestrial LoRaWAN	Multi-armed bandit–based parameter selection	Empirical packet loss (no explicit fading model)	Improves energy efficiency and delivery by learning optimal LoRa parameters	Not designed for maritime environments; does not model Rayleigh fading or sea dynamics.
(Leonardi et al., 2025)	Terrestrial LoRaWAN	Deep learning–based ADR (SF, TX power)	Log-distance / empirical channel	Enhances reliability compared to standard ADR using deep learning	Limited to ADR parameters; no joint SF–BW–CR ACM and no maritime channel modelling
(Ghoshal et al., 2024)	Maritime IoT (ships, offshore edge)	AI-based task offloading and energy–latency optimization	Abstracted network model (no PHY fading model)	Proposes an ensemble neural network for energy-efficient and low-latency task offloading in maritime MIoT	Does not address LoRaWAN PHY-layer adaptation (SF, BW, CR); no channel-aware ACM or fading-aware analysis.
(Al-Gumaei et al., 2022)	Terrestrial LoRaWAN	Improved rule-based ADR	Empirical/static channel assumptions	Faster convergence and stability than standard ADR	Slow reaction to fast channel variations; not suitable for highly dynamic maritime links
(Arratia et al., XXXX)	General LoRa (non-LoRaWAN)	Adaptive modulation using learning	AWGN / simplified channel	Demonstrates learning-based adaptation benefits	Not LoRaWAN-compliant; ignores duty-cycle, feedback, and maritime fading
This Work	Maritime LoRaWAN	ACM (SF, CR, BW)	Rayleigh fading and noise	Lightweight, real-time PHY adaptation maximizing effective throughput under fading	Does not yet include sea-surface reflection, ducting, or experimental validation (future work)

Table 2. List the parameters associated with each configuration level.

Level	SF	BW (kHz)	CR	Payload (bytes)	ToA (ms)
1	7	250	4/5	100	75.8
2	8	125	4/6	100	205.8
3	9	125	4/6	100	370.7
4	10	125	4/7	100	740.3
5	11	125	4/8	100	1480.7
6	12	125	4/8	100	2961.4

conditions. These values were extracted from the ToA provided by (Bagwari et al., 2022) with standard LoRa parameters for each SF, CR, and BW.

$$ToA = T_{preamble} + T_{payload} \tag{1}$$

where;

Preamble duration:

$$T_{preamble} = \left(\eta_{preamble} + 4.25\right) \times T_{sym} \tag{2}$$

Payload duration

$$T_{payload} = N_{payload} \times T_{sym} \tag{3}$$

Symbol duration:

$$T_{sym} = \frac{2^{SF}}{BW} \tag{4}$$

Number of payloads

$$N_{payload} = 8 + \max\left(\left(\left\lceil \frac{8 \times PL - 4 \times SF + 28 + 16 \times CRC - 20 \times IH}{4 \times (SF - 2 \times DE)} \right\rceil\right) \times (CRC + 4), 0\right) \tag{5}$$

Parameters: PL is the payload length in bytes, IH means implicit header mode 1 if the header is disabled (implicit mode) and 0 if the header is enabled. DE means data rate optimization is enabled and is 1 if low DE is enabled and 0 otherwise; $\eta_{preable}$ is usually 8 symbols but can be more (Bagwari et al., 2022).

The ToA calculations shown in Equations (1)–(5) help to understand the duration each message takes to transmit in each configuration level. Equation (1) calculates the total transmission time as the sum of payload durations and preamble. In Equation (2), 8 standard symbols plus 4.25 extra symbols are included in the preamble to help the receiver sync properly. The payload duration in Equation (3) depends on the number of payload symbols, which Equation (5) calculates from the payload length, CF, CR, and header settings. Lastly, symbol duration (4) increases exponentially with SF while decreasing linearly with BW. Therefore, higher spreading factors like SF12 take so much longer to transmit than SF7, even for the same message size.

3.3. PHY simulation

This subsection presents the physical layer simulation scenario adopted for performance assessment of the proposed ACM scheme in maritime environments. The simulation includes important processes such as channel coding, interleaving, CSS modulation, Rayleigh fading, and SNR-based feedback control, which simulate a real LoRaWAN PHY chain and provide a way to measure PER, throughput, and efficiency across different SNR levels. Figure 2 illustrates the PHY architecture.

3.3.1. Transmitter model

Let $b = \{b_1, b_2, \ldots\ldots. b_k Let\}$ be the source binary input sequence of length k. The source data is provided to an FEC encoder, which maps k bits to n coded bits with;

$$CR = \frac{k}{n} \tag{6}$$

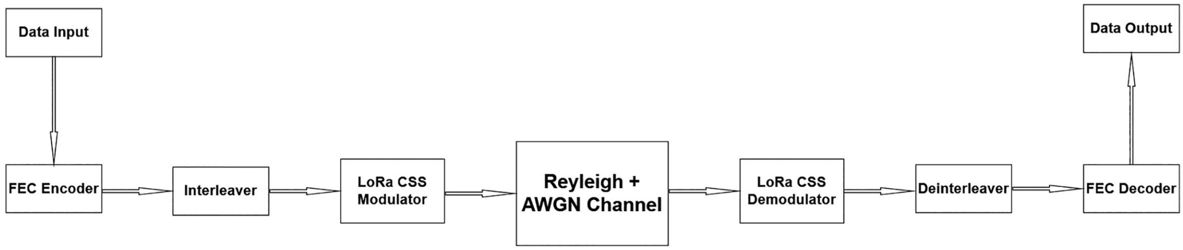

Figure 2. LoRa PHY simulation block design.

The coded information is interleaved to flatten the burst errors, generating a sequence c. The interleaved bits are modulated with CSS modulation, spreading the signal across a large bandwidth with a linearly increasing or decreasing chirp. The total number of signals or symbols

$$M = 2^{SF} \tag{7}$$

where SF determines the number of chirps per symbol, and each symbol is conveyed using one of M chirps, leading to robust communication via spreading and frequency shifting (Hanif and Nguyen, 2021).

3.3.2. Channel model

Rayleigh fading over additive white Gaussian noise (AWGN) is used in a maritime wireless channel to transmit the signal to the receiver. With the baseband-equivalent received signal

$$r(t) = h(t).s(t) + n(t) \tag{8}$$

where:

$r(t)$ Represents the received signal, which is the signal and noise in its faded form.

$s(t)$ is the transmitted signal at time t

$h(t) \sim CN(0, \sigma^2)$ represents the Rayleigh fading modelled as a complex Gaussian random variable with variance σ^2 and zero mean.

$n(t) \sim CN(0, N_0)$ represents a complex Gaussian white noise with power spectral density N_0 and zero mean.

In (8), AWGN/WGN is used as a baseline model to isolate and clearly quantify the impact of small-scale fading on LoRaWAN performance. While AWGN is an idealized model, it remains a standard assumption in PHY-level evaluation because it enables reproducible benchmarking and highlights the relative gains due to the proposed adaptation strategy. In real maritime environments (especially near ports), additional non-ideal disturbances may appear, such as narrowband interference and impulsive noise. Extending the study to more complex noise/interference models (e.g. impulsive noise models such as Middleton Class-A or α-stable noise, and explicit co-channel interference) is a meaningful direction for future work. It will likely refine the SNR thresholds and the mode-switching behaviour for highly contaminated spectra.

The instantaneous SNR is denoted by γ:

$$\gamma = \frac{|h(t)|^2.P_t}{N_0} \tag{9}$$

where $|h(t)|^2$ is the power gain of the fading channel at time t, P_t Is the signal power transmitted, and N_0 is the noise power spectral density.

This channel is modelled as a Rayleigh flat fading channel with AWGN. Rayleigh fading captures the multipath fading of the channel, and the AWGN models the thermal noise present in the background and provides a realistic relationship between packet error rates and throughput (Li et al., 2024).

3.3.3. Receiver processing

At the receiving end, the signal is coherently demodulated by a bank of adaptive matched filters chosen as chirp basis functions. The estimated data sequence is recovered from the demodulated signal after deinterleaving and through the FEC decoder. From the Cyclic Redundancy Check (CRC) checking, a PER is derived, which depends on the PHY mode in use and the channel SNR.

3.3.4. SNR feedback and ACM decision logic

An important part of this system is the feedback loop for adapting LoRa PHY parameters. Upon the receipt of each successful packet, the receiver calculates the average SNR over the last packet duration. It feeds back the estimate to the transmitter in an acknowledgement (ACK) message. According to this feedback, the transmitter performs ACM, which is to select the best configuration level (combination of SF_CR_BW) from the designed configuration level. The intention is to achieve maximum throughput, with PER being below a certain target. The decision-making process for transitioning between configuration levels is regulated by SNR thresholds, which define the boundaries for each configuration level. Specifically, the selection rule is defined as:

$$\gamma^{th}(i) < \gamma \leq \gamma^{th}(i+1) \tag{10}$$

The level i of the corresponding configuration is chosen when γ lies between certain SNR values.

3.3.5. System-level flow

To guarantee communication with time-varying and high-cost maritime channels, an entire round of transmission and adaptation process progresses as follows;

1. The transmitter starts with a preset default mode,
2. The packet is encoded, modulated, and transmitted
3. The packet is demodulated/decoded at the receiver
4. SNR is estimated, and feedback is transmitted
5. The ACM algorithm adjusts the configuration if it is needed.

3.4. Feedback and retransmission mechanism

The retransmission scheme is based on a stop-and-wait policy over ACK. At the end of each transmission, the receiver sends back an ACK including the measure of the SNR. If the packet fails the CRC check, retransmission is induced. The effective throughput $T(\gamma)$ for each configuration is computed in the following form, taking into account PER and ToA.

$$T(\gamma) = \frac{\left(1 - PER(\gamma)\right) \times PayloadBits}{ToA} \tag{11}$$

where $PER(\gamma)$ is PER at SNR γ, and PayloadBits is the number of bits in the payload.

3.5. Link-quality metrics and performance modelling

To formalize adaptation, the gateway estimates received signal strength and signal-to-noise ratio per uplink packet. Let $\mathrm{P_r}$ denote the received signal power and N_0 the noise power spectral density. For bandwidth BW, the noise power is $\mathrm{N = N_0 \cdot BW}$, and the (linear) SNR estimate is $\hat{\gamma} = \mathrm{P_r/N}$ (often reported in dB in LoRa receivers). RSSI is treated as a received power indicator and can be used jointly with SNR when needed.

Packet error rate is modelled as a function of SNR and PHY mode, $\mathrm{PER_m}(\gamma)$, obtained from a simulation under the assumed maritime channel model. The packet delivery ratio is then

$$\mathrm{PDR_m}(\gamma) = 1 - \mathrm{PER_m}(\gamma) \tag{12}$$

For payload size L bits and time-on-air ToA_m, the instantaneous throughput under mode m can be expressed as

$$\mathrm{G_m}(\gamma) = \frac{\mathrm{L}}{\mathrm{ToA_m}} \times \left(1 - \mathrm{PER_m}(\gamma)\right) \tag{13}$$

When retransmissions are enabled, the expected number of transmissions for success is

$$\mathrm{E[N_{tx}]} = 1/\mathrm{PDR_m}(\gamma) \tag{14}$$

(geometric assumption), giving an effective throughput (successful bits per second)

$$\mathrm{T}_{\mathrm{m}}^{\mathrm{eff}}(\gamma) = \frac{\mathrm{L}}{\mathrm{ToA}_{\mathrm{m}} \times \mathrm{E}[\mathrm{N}_{\mathrm{tx}}]} = \frac{\mathrm{L} \times \mathrm{PDR}_{\mathrm{m}}(\gamma)}{\mathrm{ToA}_{\mathrm{m}}} \tag{15}$$

These expressions motivate selecting the mode that maximizes $\mathrm{T}_{\mathrm{m}}^{\mathrm{eff}}(\gamma)$ or $\mathrm{G}_{\mathrm{m}}(\gamma)$ while satisfying reliability constraints.

3.6. SNR-based ACM switching algorithm

Real-time SNR feedback is used for on-the-fly selection of the optimal PHY configuration implemented by the ACM strategy. Upon receipt of each packet, the receiver estimates the SNR and returns the value in the ACK. The transmitter applies a set of predetermined switching thresholds to determine the configuration level for achieving maximized expected throughput. This technique dramatically increases throughput robustness against static setups, especially in rapidly varying nautical environments.

3.6.1. Simulation setup

A Monte Carlo simulation framework, developed in-house, was used to assess the performance of the proposed ACM scheme. The maritime environment was modelled as a Rayleigh flat-fading channel in the presence of AWGN. Simulations were conducted for –20 dB to +10 dB SNR at 1 dB SNR intervals. 1000 iterations were run at each SNR point to gain statistical significance. The parameters of the LoRa PHY configurations that we used are given in Table 2, employing a frame size of 100 bytes and a carrier frequency of 868 MHz. It was assumed that the feedback channel was perfect: perfect reporting between the sources and transceiver with no delay, no error, and no noise. All simulations were conducted with MATLAB R2023a. No Doppler spread or mobility-related factors were considered at this stage, which is left as a topic of our future work.

3.6.2. ACM control algorithm flowchart

Figure 3 illustrates that the decision tree tests the SNR thresholds in a sequence (>7 dB, >4 dB, >0 dB, >–3 dB, >–7 dB) to find the best configuration out of the six pre-defined levels. These go from SF7/CR4:5/BW250 for good channels to SF12/CR4:8/BW125 for dirty links. Every decision path dynamically reconfigures the transmission parameters for the trade-off between throughput and reliability. This dynamic reconfiguration allows ACM to achieve as much as 10^3 times the throughput gain over static configurations under dynamic maritime environments.

3.6.2.1. Threshold selection rationale. The SNR thresholds were determined via offline calibration using the PER-versus-SNR behaviour of each candidate PHY mode under the assumed maritime fading model. Specifically, for each mode $m \in \{1, \dots, M\}$, the PER (γ) curve was obtained (simulation-based), and switching points were set such that the selected mode maximizes expected throughput while satisfying a target reliability constraint (e.g. $\mathrm{PDR} \geq \mathrm{PDR}_{\mathrm{target}}$ or equivalently $\mathrm{PER} \leq \mathrm{PER}_{\mathrm{target}}$). We used five levels primarily to (i) align with the practical LoRaWAN SF7–SF12 operating set and (ii) keep the decision logic and feedback overhead lightweight, which reduces mode oscillation risk in rapidly varying channels. More levels (finer quantization) are possible; however, they increase switching sensitivity and typically require stronger hysteresis/hold-time logic, while providing diminishing performance gains beyond a moderate number of modes.

3.6.3. Pseudocode

The pseudocode in Table 3 gives the logic of the decision-making procedure employed by the ACM scheme in choosing the best LoRaWAN physical layer configuration in real-time, given instantaneous SNR feedback. The current SNR is then classified under one out of six known ranges: each range implies a specific triple combination of SF, CR, and BW. The objective is to maximize throughput by maintaining a target PER under time-varying maritime channel conditions.

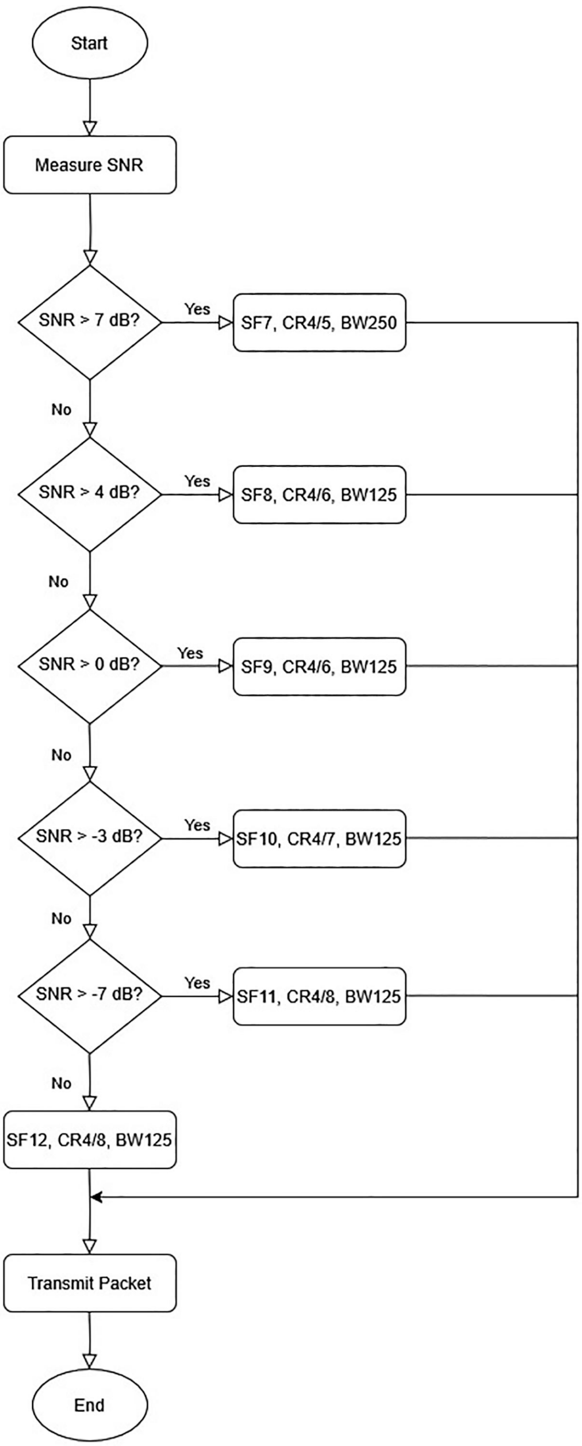

Figure 3. LoRa SNR-based parameter selection flowchart.

3.6.4. Graphical framework of the proposed ACM scheme

Figure 4 presents the graphical framework of the proposed adaptive coding and modulation (ACM) scheme for maritime LoRaWAN. In the uplink, the end device (boat node) transmits a LoRa packet that is subject to marine fading and noise. At the gateway, the received signal quality is estimated (SNR and, optionally, RSSI) and a smoothing filter (e.g. a window average or an exponential moving average) is applied to mitigate short-term fluctuations. The ACM decision block then maps the filtered SNR to a PHY mode index using pre-defined thresholds (with hysteresis and/or a minimum hold time to avoid rapid toggling). The selected mode (SF, BW, CR) is communicated back to the end device (e.g. using a

Table 3. SNR-based ACM switching algorithm.

Step	Description
1	**Input:** Receive the measured SNR value γ from receiver feedback
2	**Initialize configuration levels L_1 to L_6 as:** L_1 = (SF7, CR4/5, BW250), L_2 = (SF8, CR4/6, BW125), L_3 = (SF9, CR4/6, BW125), L_4 = (SF10, CR4/7, BW125), L_5 = (SF11, CR4/8, BW125), L_6 = (SF12, CR4/8, BW125).
3	**Initialize SNR thresholds:** $\gamma_1 = 7$ dB, $\gamma_2 = 4$ dB, $\gamma_3 = 0$ dB, $\gamma_4 = -3$ dB, $\gamma_5 = -7$ dB.
4	If $\gamma > \gamma_1$, select configuration level L_1.
5	Else if $\gamma > \gamma_2$, select configuration level L_2.
6	Else if $\gamma > \gamma_3$, select configuration level L_3.
7	Else if $\gamma > \gamma_4$, select configuration level L_4.
8	Else if $\gamma > \gamma_5$, select configuration level L_5.
9	Otherwise, select configuration level L_6.
10	**Output:** Selected configuration level L for the current SNR.
11	Update transmitter parameters according to the selected configuration and proceed with packet transmission.

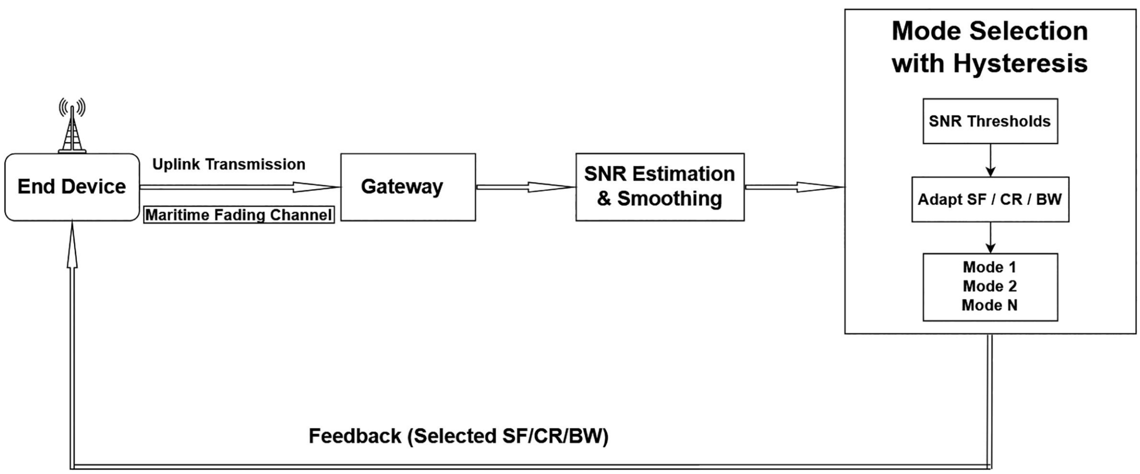

Figure 4. ACM-LoRaWAN framework: uplink transmission, SNR-based mode selection with hysteresis, and feedback to the end device.

compact mode index in a downlink/ACK or MAC command) and the device applies the new PHY configuration for subsequent transmissions.

3.7. Application scenario: Adaptive LoRaWAN in boat tracking

One practical application of the proposed ACM scheme is in coastal boat surveillance systems, where fishing boats and small transport ships are equipped with GPS units based on LoRaWAN devices to report their location and speed to a shore-based gateway periodically. Unlike the traditional systems with fixed transmit parameters, the proposed ACM scheme makes each boat dynamically select its physical layer settings based on the received signal quality.

The tracker (when the boat is onshore and under good channel conditions) can transmit with a high-throughput setting, which in turn reduces airtime. As the boat enters heavy sea states or disruptions such as increased range and environment, the system automatically switches to more robust configurations to maintain link availability. This adaptation mechanism will guarantee continuous tracking of boats at various distances and sea states while maintaining low retransmissions and power consumption. This technique permits robust maritime visibility and operational safety with neither manual reintroduction nor a priori knowledge of the environment.

3.8. Real-time feasibility and computational complexity

The proposed ACM decision mechanism is lightweight: it performs (i) optional SNR smoothing (one multiplication and addition per packet for EMA for a small fixed window), followed by (ii) a threshold comparison and a table lookup to obtain the next PHY mode. For K thresholds (here $K = 5$), the decision cost is O(K), which is effectively constant time for embedded operation. Memory requirements are minimal, consisting of a small PHY mode table (SF, BW, CR, ToA) and a few state variables, such as γ, the last mode index, and the hold-time counter.

From a timing perspective, LoRa packet time-on-air is typically on the order of tens to thousands of milliseconds, depending on SF/BW/payload, whereas the ACM computation requires only a few arithmetic operations and comparisons; therefore, the decision can be computed well within the inter-packet interval, supporting real-time adaptation at the packet timescale. Future work will include implementation-level benchmarking on representative LoRaWAN microcontrollers to report measured execution time and energy overhead.

4. Results and discussion

This section provides results to verify the performance of the ACM scheme proposed in comparison with a fixed LoRaWAN configuration over the maritime channel model. The analysis begins with PER under Rayleigh fading, continues with throughput evaluation for fixed configurations and lastly, performance assessment of the ACM scheme.

4.1. Performance metrics

In addition to throughput, we report reliability, energy, and latency metrics. Packet delivery ratio (PDR) is defined as

$$\mathrm{PDR} = 1 - \mathrm{PER} \tag{16}$$

where PER is obtained per PHY mode under the channel model. Effective throughput accounts for successful delivery and is computed in Equation (15).

Energy consumption is evaluated using energy-per-successful-bit, E_b^{succ}, approximated as

$$\mathrm{E_b^{succ}} \approx \frac{\mathrm{P_t} \times \mathrm{ToA} \times \mathrm{E}[\mathrm{N_{tx}}]}{\mathrm{L}} \tag{17}$$

where $\mathrm{P_t}$ is transmitting power and $E[N_{tx}]$ is the expected number of transmissions for success (derived from PDR). Latency is reported as the expected delivery time, approximated as

$$\mathrm{E}[\mathrm{T_{lat}}] \approx \mathrm{ToA} \times \mathrm{E}[\mathrm{N_{tx}}] + \mathrm{T_{ack}} \tag{18}$$

where $\mathrm{T_{ack}}$ accounts for ACK/receive window timing if confirmed messages are assumed (set $\mathrm{T_{ack}} = 0$ for unconfirmed traffic). These metrics jointly characterize the trade-off between throughput, reliability, energy, and timeliness in maritime LoRaWAN links.

4.2. Per under Rayleigh fading

Figure 5 shows the PER versus SNR for LoRa SF7–SF12 under Rayleigh fading. The curves have a sigmoidal shape, showing that each step up in SF improves sensitivity by about 2–3 dB. For instance, SF7 needs roughly +8 dB to achieve reliable performance (PER $<$ 0.1), while SF12 can operate effectively at SNRs as low as –12 dB. The broader transition regions of $\sim$5 dB from PER $=$ 0.9 to 0.1 are characteristic of Rayleigh fading, in contrast to sharper transitions in AWGN channels. These behaviors define critical operational thresholds for selecting optimal spreading factors in adaptive modulation strategies under dynamic wireless conditions.

4.3. Throughput for fixed configurations

Figure 6 represents throughput versus SNR for constant LoRa settings (SF7–SF12) with a 100-byte payload. For SNR $>$ 5 dB, SF7 provides the highest throughput (27 kbps), and for the other SFs, the range increases by 2–3 dB for the previous SFs at the cost of a worse throughput. The waterfall curve reveals the trade-off between data rate and robustness. Hence, adaptive system designs are essential to keep the performance at a satisfactory level over different channel characteristics.

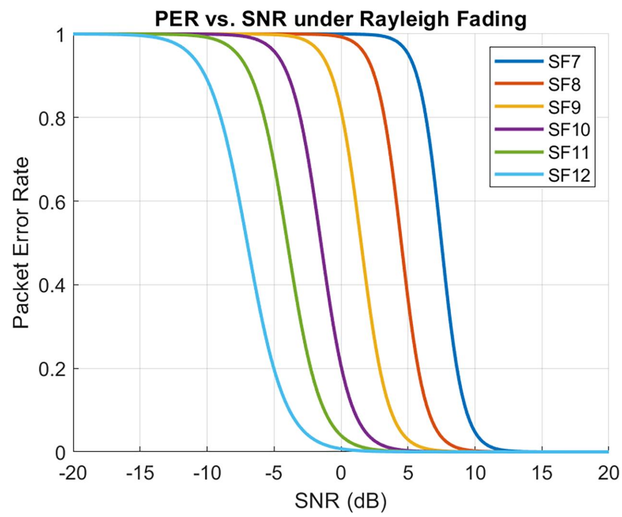

Figure 5. PER vs. SNR for LoRaWAN configurations under Rayleigh fading.

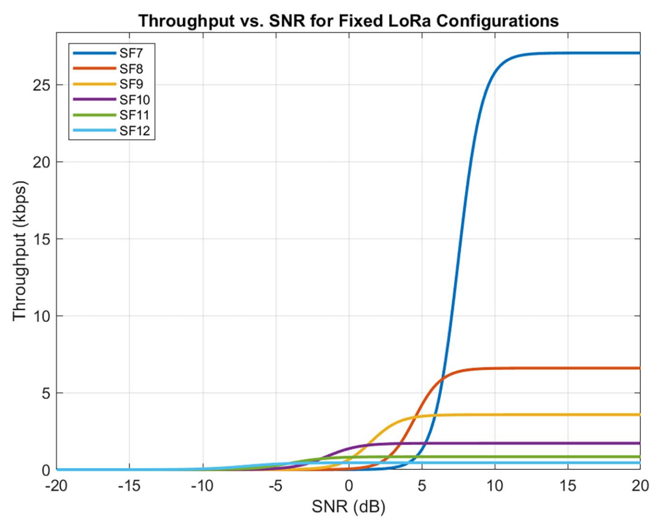

Figure 6. Throughput vs. SNR for fixed LoRaWAN configurations.

4.4. Adaptive coding and modulation performance

4.4.1. ACM performance envelope

Figure 7 shows the ACM throughput envelope (black line) mapped over fixed SF performance (dashed). The envelope relates to the maximum achievable throughput at each SNR as a result of dynamic SF selection. Shaded areas represent optimal SFs, ranging from below −10 to 5 dB (SF12 to SF7). The step-wise pattern accentuates throughput transitions as ACM adjusts over a 40 dB SNR span, ensuring the reliability of the link down to −20 dB and achieving ∼27 kbps at high SNR.

4.4.2. Throughput gain of ACM vs. fixed SF7

Figure 8 illustrates the throughput gain obtained by ACM over a fixed SF7 configuration over a variety of SNRs. At high SNR (over 8 dB), the gain is 1 since both the ACM and fixed schemes choose SF7, which is optimal for good channel conditions. However, ACM improves over fixed SF7 by a large margin as the SNR becomes lower with 100 at −2dB and up to 1000(10^3) at −5 dB and beyond by selecting more robust spreading factors. SF7 by itself, on the other hand, is unusable under low SNR due to large error rates. The results show that ACM can achieve quality of service and link reliability even in a harsh wireless environment where a fixed configuration cannot succeed.

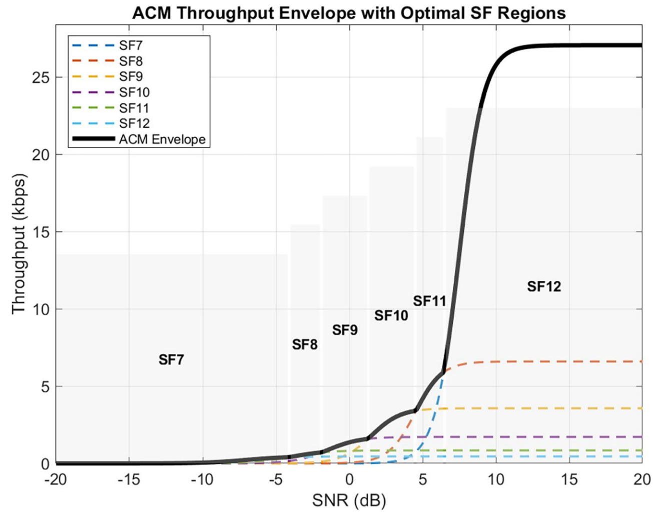

Figure 7. ACM throughput envelope with optimal SF regions.

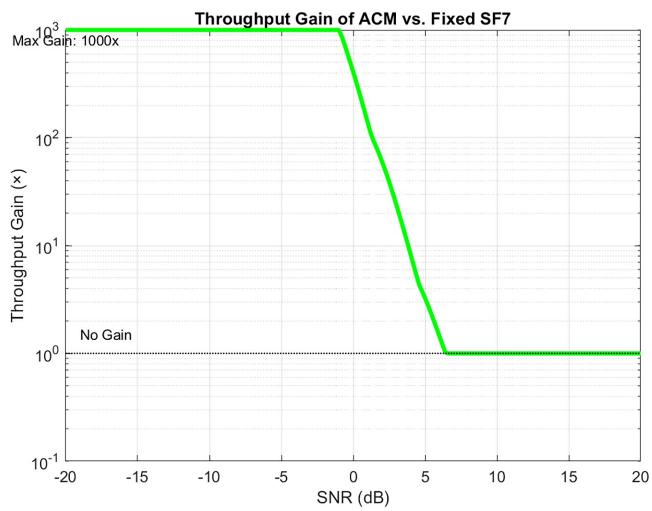

Figure 8. Throughput gain achieved by ACM vs. fixed SF7.

The real-world implications of this gain are vital for maritime IoT deployments. At −5 dB SNR, which often happens in rough maritime conditions or storms, a fixed SF7 setup would lose connection, require multiple retransmissions or possibly fail entirely. The ACM system, on the other hand, switches automatically to SF10 or SF11, keeping the data flowing even in tough conditions. This kind of flexibility helps maritime monitoring systems keep running when fixed setups would fail, avoiding data loss during emergencies or sudden weather changes.

4.4.3. Energy efficiency and spectral efficiency

Figure 9 shows the energy per bit (μJ/bit) comparison over constant LoRa SFs (SF7–SF12) with the ACM scheme. For fixed configurations, the energy costs are found to increase rapidly at low SNR, primarily due to retransmissions. In contrast, ACM can maintain a very low energy usage by choosing the best operating configuration at all SNR levels. Such energy-aware trade-offs are of great interest in IoT scenarios relying on battery-operated devices in non-ideal or time-varying channel conditions (Sarkar et al., 2021).

We plot the spectral efficiency (in bits/s/Hz) when applying fixed LoRa settings and the proposed adaptive ACM scheme in Figure 10. The ACM envelope (black) has a stair-step shape that reflects its preference for more spectrally efficient spreading factors as the SNR increases. At high SNR, SF7 is chosen by the system, and the spectral efficiency achieves close to 0.11 bits/s/Hz. For low SNRs (up to −15 dB), less efficient but more reliable SFs are selected to satisfy connectivity. This adaptive behavior

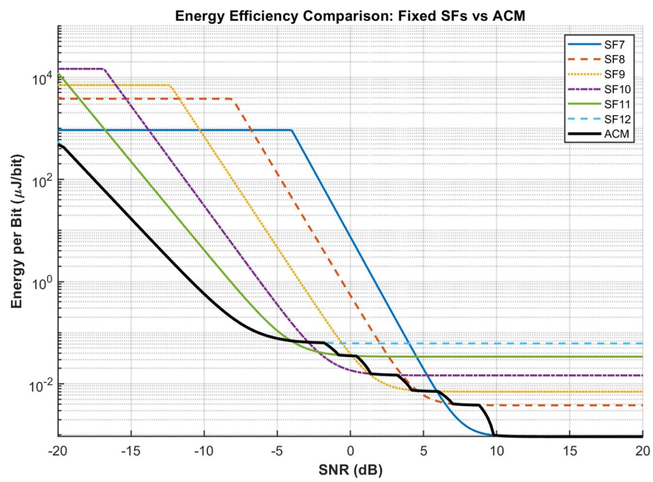

Figure 9. Variation of energy efficiency to SNR for LoRa configurations.

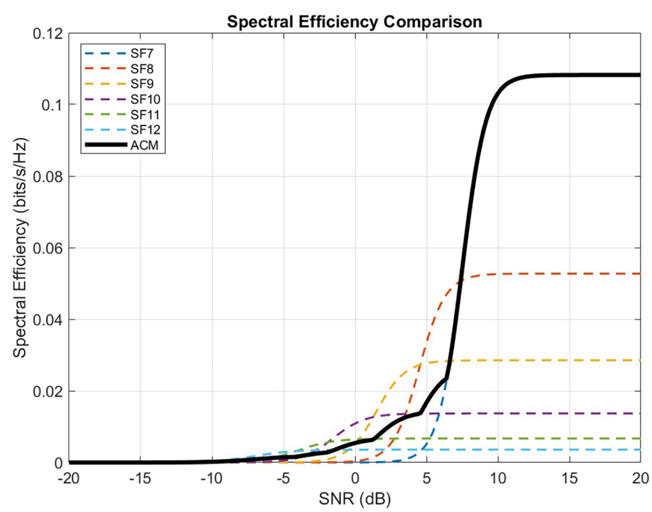

Figure 10. Variation of spectral efficiency to SNR for LoRa configurations.

allows for the efficient use of bandwidth resources as well as the reliability of links over various and changing propagation environments.

4.4.3.1. Measurement frequency and smoothing. In this study, the gateway updates the link-quality estimate once per received uplink packet (i.e. per transmission opportunity). To improve robustness against short fades, the instantaneous SNR estimate can be smoothed using a window of the last M packets or an exponentially weighted moving average (EMA),

$$\overline{\gamma}[n] = \alpha\gamma[n] + (1-\alpha)\overline{\gamma}[n-1] \tag{19}$$

where $\alpha \in (0, 1]$. The ACM decision is then made using $\overline{\gamma}[n]$ and applied for subsequent transmissions. To prevent rapid toggling in fast-varying maritime conditions, hysteresis margins and/or a minimum hold time (minimum number of packets before switching again) can be enforced.

4.4.3.2. Energy implication. The decision step is computationally trivial (a few comparisons and a table lookup). The dominant energy cost for LoRaWAN nodes is radio ToA and retransmissions; therefore, ACM generally reduces energy consumption by avoiding repeated failed transmissions in poor channel states and by selecting shorter-ToA modes when channel quality permits.

4.4.4. Baseline comparison with ADR-family schemes

The proposed ACM scheme is compared with standard LoRaWAN ADR, in which only the SF is adjusted based on the long-term average SNR, while bandwidth and coding rate remain fixed. Because ADR relies on averaged channel conditions, it responds slowly to rapid fading and short-term variations. In this study, ADR performance is evaluated by selecting the steady-state SF corresponding to each average SNR and computing metrics using the same PER and ToA models as ACM. An ADR-Enhanced variant with a shorter averaging window is also included, but its steady-state performance is identical under the assumed channel model. Figures 11–13 show effective throughput, PDR, and energy per successful bit for fixed PHY settings, ADR-based schemes, and ACM. While ADR improves reliability relative to fixed configurations, its SF only adaptation limits performance. In contrast, ACM jointly adapts SF, BW, and CR based on instantaneous link quality, achieving higher throughput and better energy efficiency across a wider SNR range while maintaining the target reliability.

It should be noted that ADR and ADR-Enhanced results represent steady-state behaviour under average SNR conditions, whereas the proposed ACM operates on instantaneous link quality. The presented results, therefore, quantify performance limits rather than protocol-level convergence dynamics. Furthermore, the analysis focuses on physical-layer performance and does not include MAC-layer effects such as retransmissions, duty-cycle constraints, or network-level contention.

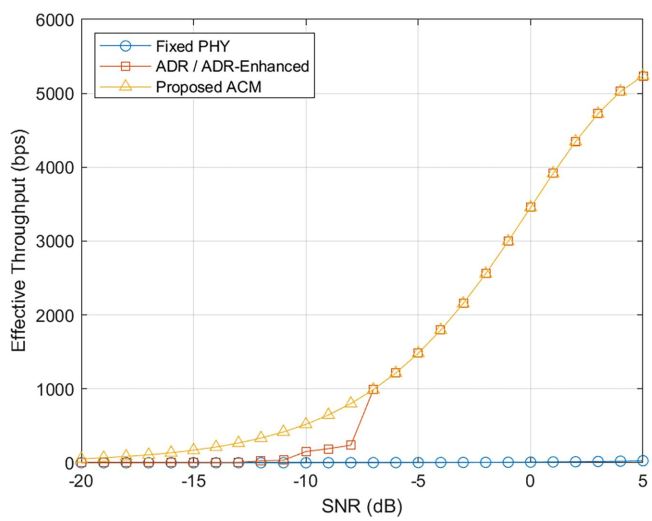

Figure 11. Effective throughput versus SNR for fixed PHY, ADR/ADR-Enhanced, and ACM.

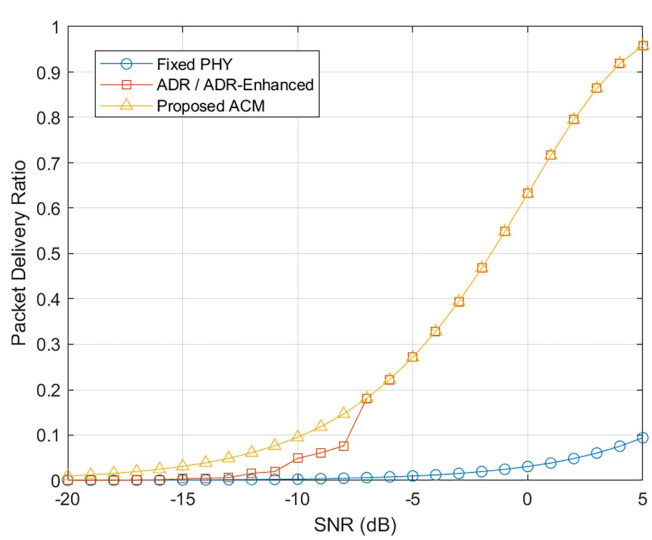

Figure 12. Packet delivery ratio versus SNR for fixed PHY, ADR/ADR-Enhanced, and ACM.

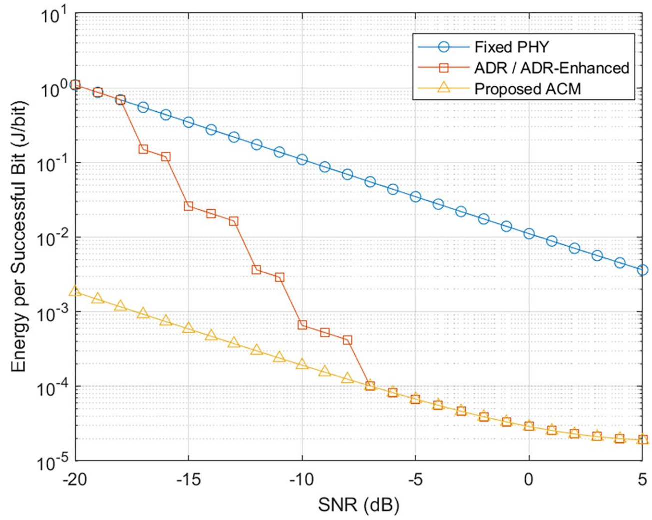

Figure 13. Energy per successful bit versus SNR for fixed PHY, ADR/ADR-Enhanced, and ACM.

4.4.4.1. Robustness definition and limits. In this article, robustness is assessed quantitatively as the ability of the scheme to sustain a target reliability level (e.g. PDR $\geq$ PDR_{target} or PER $\leq$ PER_{target}) across a wide SNR range while maximizing throughput. The proposed ACM improves robustness by switching to more resilient PHY modes (higher processing gain) when SNR degrades, thereby reducing packet failures and retransmissions. The limits of the method arise from (i) imperfect or delayed feedback in practical LoRaWAN downlinks, (ii) estimation error in SNR (especially with sparse traffic), (iii) threshold quantization and potential mode oscillation (mitigated via hysteresis/hold time), and (iv) the scope of the channel/noise model used in simulations. Incorporating additional maritime propagation effects such as two-ray sea reflection, evaporation ducting and non-Gaussian interference is left as future work.

5. Future work

In future work, experiments will be carried out to validate the ACM mechanism in a real maritime environment, while energy-aware and mobility-policy-aware, combined to achieve a better performance. The next step is to adapt the ACM framework to better reflect real maritime conditions, such as reflections off the sea surface and ducting effects, and then test it in real-world experiments. The study could also examine more complex noise and interference, such as impulsive noise (Middleton Class A or α-stable) and co-channel interference, to assess how ACM performs under realistic conditions. The methodology of cross-layer design utilizing Media Access Control (MAC) layer mechanisms, including acknowledgements, duty cycle control, and dynamic data rate, will be applied to achieve a complete network solution. The study will explore using AI techniques, such as Reinforcement Learning to predict channel conditions and Neural Networks to optimize system parameters. These methods could help the system adapt in advance by learning from past channel behavior and environmental factors. Applying AI in this way may also improve throughput and energy efficiency in maritime IoT networks. The standardization impact of these adaptive mechanisms will also be investigated and analyzed to ensure greater dissemination of such mechanisms in future commercial maritime IoT systems.

6. Conclusion

This article has proposed an ACM scheme to enhance LoRaWAN communication in maritime environments where the presence of slowly time-variant Rayleigh fading creates a major challenge to relationship reliability and effectiveness. Contrary to typical static LoRaWAN parameters, the advised approach rapidly changes core PHY configuration factors (SF, CR and BW) according to instantaneous receiver feedback to guarantee efficient communication practices in varying channel scenarios.

Through extensive Monte Carlo simulations, it was shown that the ACM system, as proposed in this article, can select more robust spreading factors dynamically to preserve communication reliability and achieve a maximum throughput gain of the order of $10^3\times$ for low-SNR when fixed SF7 settings are ineffective. This achievement demonstrates the necessity of physical layer adaptability for reliable and efficient communication for IoT applications in the maritime environment.

6.1. Limitations

The proposed ACM framework assumes an ideal feedback channel (error-free and delay-free reporting). In operational LoRaWAN, downlink duty-cycle constraints, ACK loss, and feedback delay may reduce the timeliness and accuracy of the adaptation decision. Practical implementations can mitigate this by using quantized mode indices, conservative switching margins, hysteresis and minimum hold time, and fallback default PHY modes when feedback is unavailable.

Acknowledgements

The authors thank an anonymous colleague for helpful discussions. Conceptualization, M.L.; study design, M.L. and B.M.; analysis and interpretation, M.L., B.M., J.L. and M.D.; writing original draft preparation, M.L.; critically reviewed the article, B.M., J.L., M.D. and K.M.; supervision, B.M., J.L., M.D. and K.M.; journal to which the article will be submitted, M.L., B.M., J.L., M.D. and K.M.; All authors have read and agreed to the published version of the manuscript.

Author contributions

CRediT: **Martine Lyimo**: Conceptualization, Formal analysis, Methodology, Writing – original draft; **Bonny Mgawe**: Formal analysis, Supervision, Writing – review & editing; **Judith Leo**: Formal analysis, Supervision, Writing – review & editing; **Mussa Dida**: Formal analysis, Supervision, Writing – review & editing; **Kisangiri Michael**: Formal analysis, Supervision, Writing – review & editing.

Institutional review board statement

Not applicable.

Informed consent statement

Not applicable.

Disclosure statement

No potential conflict of interest was reported by the author(s).

Funding

No funding was received for this study from any funding agency in the public, commercial or not-for-profit sector.

About the authors

Mr ***Martine Lyimo*** received his BSc in Telecommunications Engineering in 2010 from the University of Dar-es-Salaam, MSc in Embedded and Mobile Systems from the Nelson Mandela African Institution of Science and Technology in 2021; he is currently pursuing his PhD degree in Information and Communications Systems and Engineering and works as an Assistant Lecturer and researcher in the School of Computational and Communication Science and Engineering at The Nelson Mandela African Institution of Science and Technology, Arusha, Tanzania. For more than 12 years, He has been involved in several engineering projects related to ICT and Telecommunication solutions as an installer, consultant or maintenance engineer. His research interests include IoT and embedded systems, Wireless Sensor Networks (WSN), Wireless and Mobile Communication and Deep Learning.

Dr. *Bonny Mgawe* has a bachelor's and Master's Degree in Electrical Engineering (Telecommunication) from Abou Bekr Belkaid University, Algeria. Before undertaking his PhD studies at the Pan African University Institute for Science and Technology, he served two years as a data centre engineer with Tigo Tanzania. He graduated in 2019 with a specialization in signal processing and wireless communication. He is a lecturer at the Nelson Mandela African Institution of Science and Technology (NM-AIST) and a Certified Telecommunication Engineer (Level 3, P0656-RFC). His previous project, together with KMUTT (Thailand), focused on designing an antenna-based soil health assessment device for smallholder farmers. His research interests are in wireless sensors, AI applications, and signal processing.

Dr. Ing. *Judith Leo* is a Tanzanian engineer and data scientist who currently serves as a Senior Lecturer and Chairperson of the Cybersecurity and Privacy Research Theme at the School of Computational and Communication Science and Engineering (CoCSE) at the Nelson Mandela African Institution of Science and Technology (NM-AIST). She directs research and development efforts in developing hardware-accelerated innovations that span the spectrum of Artificial Intelligence (AI), embedded and mobile domains. Dr. Leo is a hands-on mentor and is very involved in coaching staff and students in using engineering principles to create viable solutions. Her research interests range from bioinformatics, data science, satellite imagery, mobile apps, and embedded systems to the IoT.

Dr. *Mussa Dida* is the Dean of the School of Computational and Communications Science and Engineering (CoCSE) at the Nelson Mandela African Institution of Science and Technology (NM-AIST) and a Senior Lecturer in the same school. He received a PhD degree in Information and Communication Systems Engineering from Beijing Institute of Technology (China) in 2017, an MSc in Telecommunications Engineering from the University of Dodoma in 2011, and a BSc in Computer Engineering and IT from the University of Dar es Salaam in 2008. He specializes in Wireless Communications, Embedded Systems, Cyber Security, and the development of IT Systems. He is now managing a project to develop an agricultural extension support system and logistics platform for farmers.

Prof. *Kisangiri Michael* is a Senior Lecturer at the Nelson Mandela African Institution of Science and Technology (NM-AIST), Tanzania, and his research focuses on wireless and mobile communications. He received his PhD in Telecommunications from Wroclaw University of Technology, Poland, in 2008. For many years now, he has been a committed academic, supervising numerous MSc and PhD projects effectively. Under his supervision, he is guiding the research work in various fields such as Information Science (Artificial Intelligence, Epidemic Control, Agriculture, Mobile Applications, etc.) and Wireless Communication (IoT, Antenna Design, Mobile Network Optimization, etc.). He is interested in IoT and Mobile communication research.

ORCID

Martine Lyimo http://orcid.org/0009-0003-8426-5187
Bonny Mgawe http://orcid.org/0000-0003-2089-485X
Judith Leo http://orcid.org/0000-0002-7420-6533
Mussa Dida http://orcid.org/0000-0002-7143-8953
Kisangiri Michael http://orcid.org/0000-0003-2534-7521

Data availability statement

The data and MATLAB code used to support the findings of this study are openly available in the ZENODO repository: https://doi.org/10.5281/zenodo.16740965 (30). The dataset contains energy efficiency, PER, throughput and spectral efficiency values for different LoRa configurations along with the adaptive coding and modulation algorithm in MATLAB format. Data are available under the Creative Commons Attribution 4.0 International (CC BY 4.0) license.

References

Al-Gumaei, Y. A., Aslam, N., Aljaidi, M., Al-Saman, A., Alsarhan, A., & Ashyap, A. Y. Nov (2022). A novel approach to improve the adaptive-data-rate scheme for IoT LoRaWAN. *Electronics (Switzerland)*, *11*(21), 3521. https://doi.org/10.3390/electronics11213521

Almarzoqi, S. A., Yahya, A., Matar, Z., & Gomaa, I. Feb (2022). Re-learning EXP3 multi-armed bandit algorithm for enhancing the massive IoT-LoRaWAN network performance. *Sensors*, *22*(4), 1603. https://doi.org/10.3390/s22041603

Alqurashi, F. S., Trichili, A., Saeed, N., Ooi, B. S., & Alouini, M.-S. (2022). Maritime communications: A survey on enabling technologies, opportunities, and challenges. http://arxiv.org/abs/2204.12824

Al-Sammak, K. A., Al-Gburi, S. H., Marghescu, I., Drăgulinescu, A.-M. C., Marghescu, C., Martian, A., Al-Sammak, N. A. H., Suciu, G., & Alheeti, K. M. A. Feb (2025). Optimizing IoT energy efficiency: Real-time adaptive algorithms for smart meters with LoRaWAN and NB-IoT. *Energies (Basel)*, *18*(4), 987. https://doi.org/10.3390/en18040987

Arratia, B., Rosas, E., Calafate, C. T., Cano, J.-C., Cecilia, J. M., & Manzoni, P. AlLoRa: empowering environmental intelligence through an advanced LoRa-based IoT solution. https://ssrn.com/abstract=4482080
Bagwari, S., Roy, A., Gehlot, A., Singh, R., Priyadarshi, N., & Khan, B. (2022). LoRa based metrics evaluation for real-time landslide monitoring on IoT platform. *IEEE Access*, *10*, 46392–46407. https://doi.org/10.1109/ACCESS.2022.3169797
Cheng, S., & Wang, X. Apr (2025). Analysis of maritime wireless communication connectivity based on CNN-BiLSTM-AM. *Electronics (Switzerland)*, *14*(7), 1367. https://doi.org/10.3390/electronics14071367
Durlik, I., Miller, T., Cembrowska-Lech, D., Krzemińska, A., Złoczowska, E., & Nowak, A. (2023). Navigating the sea of data: A comprehensive review on data analysis in maritime IoT applications. *Multidisciplinary Digital Publishing Institute (MDPI)*, *13*(17), 9742. https://doi.org/10.3390/app13179742
Farhad, A., Kim, D. H., Subedi, S., & Pyun, J. Y. Nov (2020). Enhanced Lorawan adaptive data rate for mobile internet of things devices. *Sensors (Switzerland)*, *20*(22), 6466. https://doi.org/10.3390/s20226466
Ghoshal, S. C., Hossain, M. M., Das, B. C., Roy, P., Razzaque, M. A., Azad, S., Hassan, M. M., Savaglio, C., & Fortino, G. (2024). VESBELT: An energy-efficient and low-latency aware task offloading in Maritime Internet-of-Things networks using ensemble neural networks. *Future Generation Computer Systems*, *161*, 572–585. https://doi.org/10.1016/j.future.2024.07.034
Guerra, R. R., Vizziello, A., Savazzi, P., Goldoni, E., & Gamba, P. Apr (2024). Forecasting LoRaWAN RSSI using weather parameters: A comparative study of ARIMA, artificial intelligence and hybrid approaches. *Computer Networks*, *243*, 110258. https://doi.org/10.1016/j.comnet.2024.110258
Hanif, M., & Nguyen, H. H. Dec (2021). Frequency-shift chirp spread spectrum communications with index modulation. *IEEE Internet of Things Journal*, *8*(24), 17611–17621. https://doi.org/10.1109/JIOT.2021.3081703
Haq, A. U., Sefati, S. S., Nawaz, S. J., Mihovska, A., & Beliatis, M. J. (2025). Need of UAVs and physical layer security in next-generation non-terrestrial wireless networks: potential challenges and open issues. *IEEE Open Journal of Vehicular Technology*, *6*, 554–595. https://doi.org/10.1109/OJVT.2025.3525781
Leonardi, L., Iannizzotto, G., Pirri, M., Patti, G., Pirri, A., & Lo Bello, L. Nov (2025). A deep learning-based Adaptive Data Rate algorithm for LoRaWAN networks. *Internet of Things (The Netherlands)*, *34*, 101786. https://doi.org/10.1016/j.iot.2025.101786
Li, F., Shui, Y., Liang, J., Yang, K., & Yu, J. (2023). Ship-to-ship maritime wireless channel modeling under various sea state conditions based on REL model. *Frontiers in Marine Science*, *10*. https://doi.org/10.3389/fmars.2023.1134286
Li, X., Xue, X., Zhou, C., Ma, J., & Su, P. (2024). A review of UV communications for UAVs. *IEEE Open Journal of the Communications Society*, *5*, 6495–6534. https://doi.org/10.1109/OJCOMS.2024.3465028
Li, Z., Dai, J., Luan, Y., Sun, N., & Du, L. Feb (2024). LR-MPIBS: A LoRa-based maritime position-indicating beacon system. *Applied Sciences (Switzerland)*, *14*(3), 1231. https://doi.org/10.3390/app14031231
Liu, S., Zhu, L., Huang, F., Hassan, A., Wang, D., & He, Y. Jan. 01 (2023). A survey on air-to-sea integrated maritime internet of things: enabling technologies, applications, and future challenges. *Journal of Marine Science and Engineering*, *12*(1), 11. https://doi.org/10.3390/jmse12010011
Lyimo, M., Mgawe, B., Leo, J., Dida, M., & Michael, K. Mar (2026). LSTM-based deep reinforcement learning for ISI mitigation in maritime LoRaWAN. *Physical Communication*, *75*, 103063. https://doi.org/10.1016/j.phycom.2026.103063
Maleki, A., Nguyen, H. H., Bedeer, E., & Barton, R. (2024). A tutorial on chirp spread spectrum modulation for LoRaWAN: basics and key advances. *IEEE Open Journal of the Communications Society*, *5*, 4578–4612. https://doi.org/10.1109/OJCOMS.2024.3433502
Maurya, P., Hazra, A., Kumari, P., Sørensen, T. B., & Das, S. K. Feb (2025). A comprehensive survey of data-driven solutions for LoRaWAN: challenges and future directions. *ACM Transactions on Internet of Things*, *6*(1), 1–36. https://doi.org/10.1145/3711953
Parri, L., Parrino, S., Peruzzi, G., & Pozzebon, A. Jul (2019). Low power wide area networks (LPWAN) at sea: performance analysis of offshore data transmission by means of LoRaWAN connectivity for marine monitoring applications. *Sensors (Switzerland)*, *19*(14), 3239. https://doi.org/10.3390/s19143239
Pensieri, S., Viti, F., Moser, G., Serpico, S. B., Maggiolo, L., Pastorino, M., Solarna, D., Cambiaso, A., Carraro, C., Degano, C., Mainenti, I., Seghezza, S., & Bozzano, R. Nov (2021). Evaluating LoRaWAN connectivity in a marine scenario. *Journal of Marine Science and Engineering*, *9*(11), 1218. https://doi.org/10.3390/jmse9111218
Pinelo, J., Rocha, A. D., Arvana, M., Gonçalves, J., Cota, N., & Silva, P. (2023). Unveiling LoRa's oceanic reach: Assessing the coverage of the Azores LoRaWAN network from an island. *Sensors*, *23*(17), 7394. https://doi.org/10.3390/s23177394
Ruotsalainen, H., Shen, G., Zhang, J., & Fujdiak, R. May (2022). LoRaWAN physical layer-based attacks and countermeasures, a review. *Sensors*, *22*(9), 3127. https://doi.org/10.3390/s22093127
Sarkar, N. I., Singh, D. P., & Ahmed, M. (2021). A survey on energy harvesting wireless networks: Channel capacity, scheduling, and transmission power optimization. *MDPI*, *10*(19), 2342. https://doi.org/10.3390/electronics10192342
Teymuri, B., Serati, R., Anagnostopoulos, N. A., & Rasti, M. Feb (2023). LP-MAB: Improving the energy efficiency of LoRaWAN using a reinforcement-learning-based adaptive configuration algorithm. *Sensors*, *23*(4), 2363. https://doi.org/10.3390/s23042363

Wang, X., Wei, M., Wang, Y., Sun, H., & Ma, J. Jan (2023). Radar signal behavior in maritime environments: Falling rain effects. *Electronics (Switzerland)*, *13*(1), 58. https://doi.org/10.3390/electronics13010058

Xylouris, G., Nomikos, N., Kalafatelis, A., Giannopoulos, A., Spantideas, S., & Trakadas, P. (2024). Sailing into the future: Technologies, challenges, and opportunities for maritime communication networks in the 6G era. *Frontiers Media SA*. https://doi.org/10.3389/frcmn.2024.1439529

Zenodo.com (2026). Data supporting: Optimizing LoRaWAN throughput in maritime environments through ACM under Rayleigh fading. https://zenodo.org/records/16740965